

Supporting Information

Fabrication of Nickel-foam-supported Layered Zinc-Cobalt Hydroxide Nanoflakes for High Electrochemical Performance in Supercapacitors

Peng Yuan,^a Ning Zhang,^{b*} Dan Zhang,^a Tao Liu,^a Limiao Chen,^c Xiaohe Liu,^{a*} Renzhi Ma,^d Guanzhou Qiu^a

^a School of Resources Processing and Bioengineering, Central South University, Changsha, Hunan 410083, P. R. China.

* E-mail: liuxh@csu.edu.cn; Fax: +86 731-8879815

^b School of Materials Science and Engineering, Central South University, Changsha, Hunan 410083, P. R. China

* E-mail: nzhang@csu.edu.cn; Fax: +86 731-8879815

^c College of Chemistry and Chemical Engineering, Central South University, Changsha, Hunan 410083, P. R. China.

^d International Center for Materials Nanoarchitectonics (MANA), National Institute for Materials Science (NIMS), Namiki 1-1, Tsukuba, Ibaraki 305-0044, Japan.

Experimental Section

Materials Synthesis. All the chemicals were of analytical grade without further purification. In a typical preparation process, 0.5g PVP (polyvinylpyrrolidone, average molecular weight $M_w \sim 58,000$) was dissolved in 20 mL de-ionized water and 10 mL ethanol. After that, 1 mmol $\text{Co}(\text{NO}_3)_2 \cdot 6\text{H}_2\text{O}$, 0.5 mmol $\text{Zn}(\text{NO}_3)_2 \cdot 6\text{H}_2\text{O}$, and 6 mmol hexamethylenetetramine (HMT) were added to the above solution and stirred for 20 minutes. Nickel foam (2 cm \times 4 cm) was washed with acetone, 2 M HCl solution, deionized water, and absolute ethanol to ensure a clean surface. Then the cleaned nickel foam was then immersed into the above solution. The solution and nickel foam was subsequently transferred to a Teflon-lined stainless steel autoclave (40 mL in capacity). Finally, the autoclave was sealed and maintained at 100 °C for 12 h. After the autoclave cooled down to room temperature, the Ni foam coated with Zn-Co hydroxide was washed under ultrasonication and then dried at 60 °C for 2 h.

Materials Characterization. The crystal phase of the products was examined by X-ray diffraction (XRD) with Cu K α radiation ($\lambda = 1.54178$) operating at D/max2550 VB+. Fourier transform infrared (FT-IR) spectroscopy was taken on a Nicolet Nexus 670 instrument. The chemical formula of the Zn-Co hydroxides was determined by using Inductive Couple Plasma Atomic Emission Spectrometer (ICP-AES) and elemental CHNO analysis. The morphology of the as-prepared products was evaluated by FEI Helios Nanolab 600i scanning electron microscopy (SEM). Transmission electron microscopy (TEM) images, high-resolution TEM (HRTEM), scanning transmission electron microscopy (STEM), Energy Dispersive X-Ray Spectroscopy (EDX), elemental mapping, and the selected area electron diffraction (SAED) were recorded on a Titan G2 60-300 transmission electron microscope.

Electrochemical measurements. Cyclic voltammetry (CV) and galvanic charge-discharge (CD) were carried out on a Gamry Interface1000 electrochemistry workstation using a three electrode cell with 1 M KOH as the electrolyte, Ag/AgCl electrode as reference electrode, platinum wire as counter electrode and Zn-Co hydroxide nanoflakes loaded Ni foam (1.0 cm \times 1.0 cm) directly as the working electrode, respectively. The estimated mass loading of Zn-Co hydroxide nanoflakes

on Ni foam is about $0.6 \text{ mg}\cdot\text{cm}^{-2}$. The specific capacitance (C) of the electrode can be evaluated according to the following equation.

$$C = \frac{I \times \Delta t}{m \times \Delta V} \quad (1)$$

where C ($\text{F}\cdot\text{g}^{-1}$) is the specific capacitance of the electrode based on the mass of active materials, I (A) is the current during discharge process, Δt (s) is the discharge time, ΔV (V) is the potential window (here $\Delta V = 0.5 \text{ V}$), m (g) is the mass of active materials.

Additional Figures

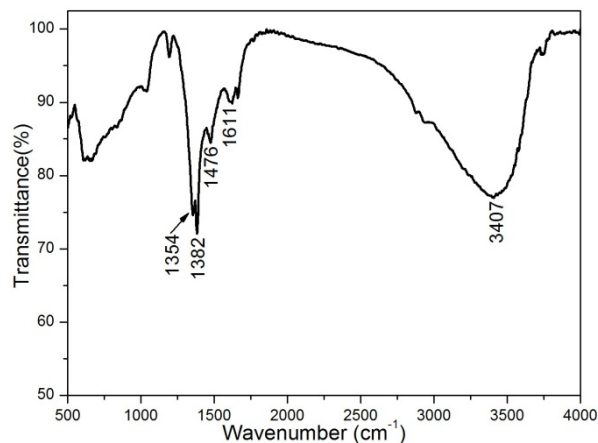


Fig. S1 FT-IR spectrum of as prepared Zn-Co hydroxide.

As illustrated in Fig. S1, the band appearing at 1382 cm⁻¹ was resulted from the interlayer NO₃⁻ anions, which come from the nitrate in synthetic process.¹ The bands at about 1354 and 1476 cm⁻¹ were characteristic of carbonate ions.² The interlayer CO₃²⁻ anions resulted from the adsorption of CO₂ from air and the possible oxidation of HMT. Furthermore, the strong and broad IR absorption at 3407 cm⁻¹ was due to the stretching vibrations of OH groups and a relatively weak absorption at 1611 cm⁻¹ was because of the bending vibration of OH groups.³ So, CO₃²⁻ and NO₃⁻ were the main charge-balancing anions located in interlayers of the layered Zn-Co hydroxide.

Table. S1 Element content of the as prepared product based on elemental analysis.

Element	Zn	Co	O	N	C	H
wt%	19.2%	34.4%	40.9%	2.7%	0.6%	2.2%

The Zn/Co ratios of the as prepared Zn-Co hydroxides were determined with ICP - AES analysis, which shows the Zn/Co ratio of ~0.50. The CHNO elemental analysis clearly demonstrated that the content of the nitrate anion and carbonate anion per formula unit is 0.22 and 0.06, respectively. Based on these results, the chemical formula was calculated to be $\text{Co}_{0.67}\text{Zn}_{0.33}(\text{OH})_{1.66}(\text{NO}_3)_{0.22}(\text{CO}_3)_{0.06} \cdot 0.44\text{H}_2\text{O}$ ($M = 114.36\text{g} \cdot \text{mol}^{-1}$).

Theoretical specific capacitance (C_t) can be evaluated according to the following

equation: $C_t = \frac{nF}{M \cdot \Delta V}$ where n is 1.34 ($= 2 \cdot 0.67$), the moles of charge transferred per mole of $\text{Co}_{0.67}\text{Zn}_{0.33}(\text{OH})_{1.66}(\text{NO}_3)_{0.22}(\text{CO}_3)_{0.06} \cdot 0.44\text{H}_2\text{O}$;

F is the Faraday constant ($= 96485 \text{ C} \cdot \text{mol}^{-1}$);

M is the molecular mass of the Zn-Co hydroxides;

ΔV is the potential range (here $\Delta V = 0.5\text{V}$).⁴

So, a theoretical specific capacitance of C_t was calculated as $2261 \text{ F} \cdot \text{g}^{-1}$.

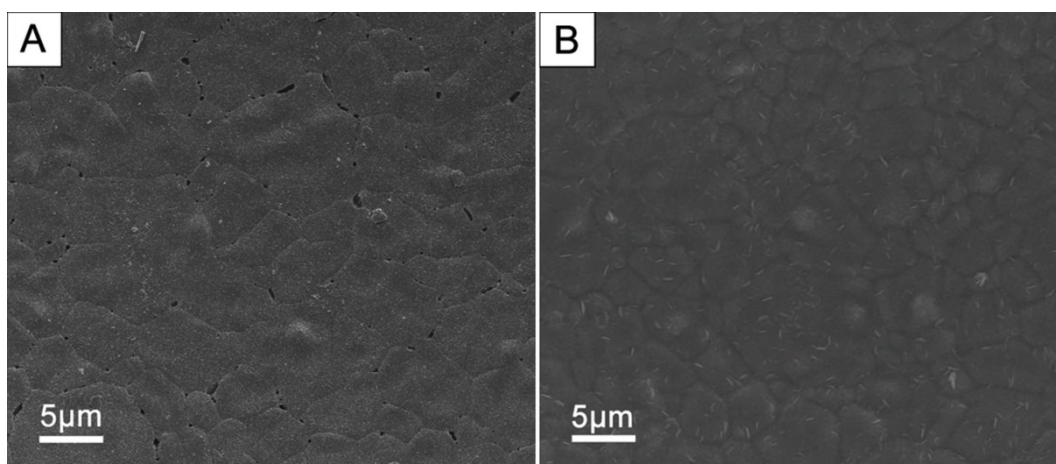


Fig. S2 SEM images of as prepared Zn-Co hydroxide by using alkali of (A) $\text{NH}_3 \cdot \text{H}_2\text{O}$ and (B) NaOH in H_2O /ethanol solvents at 100 °C for 12 h.

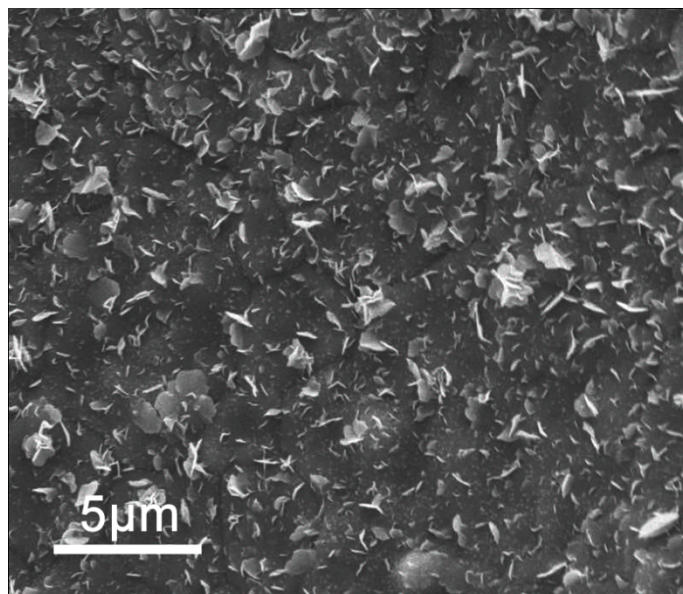


Fig. S3 SEM image of as prepared Zn-Co hydroxide at 80 °C.

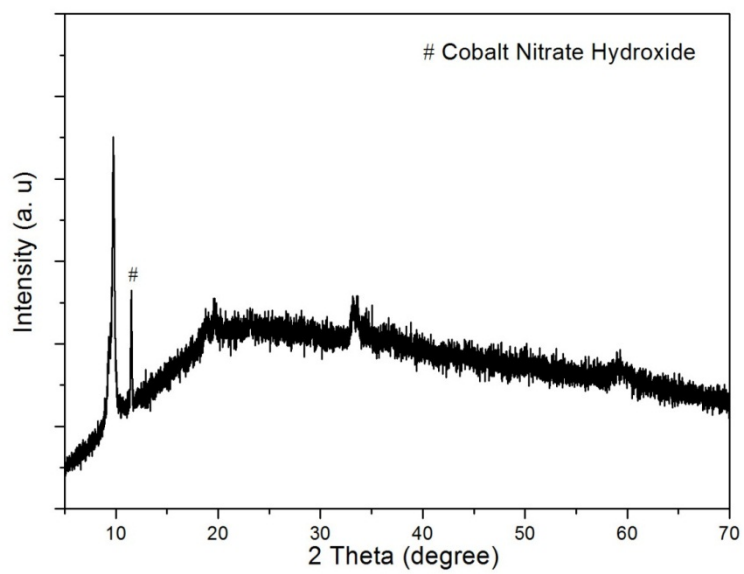


Fig. S4 XRD pattern of the sample obtained without using PVP.

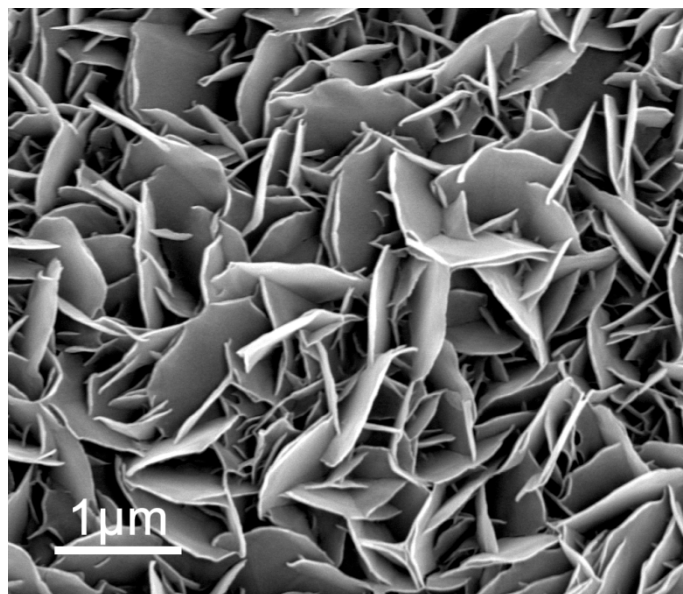


Fig. S5 SEM image of the sample obtained without using PVP.

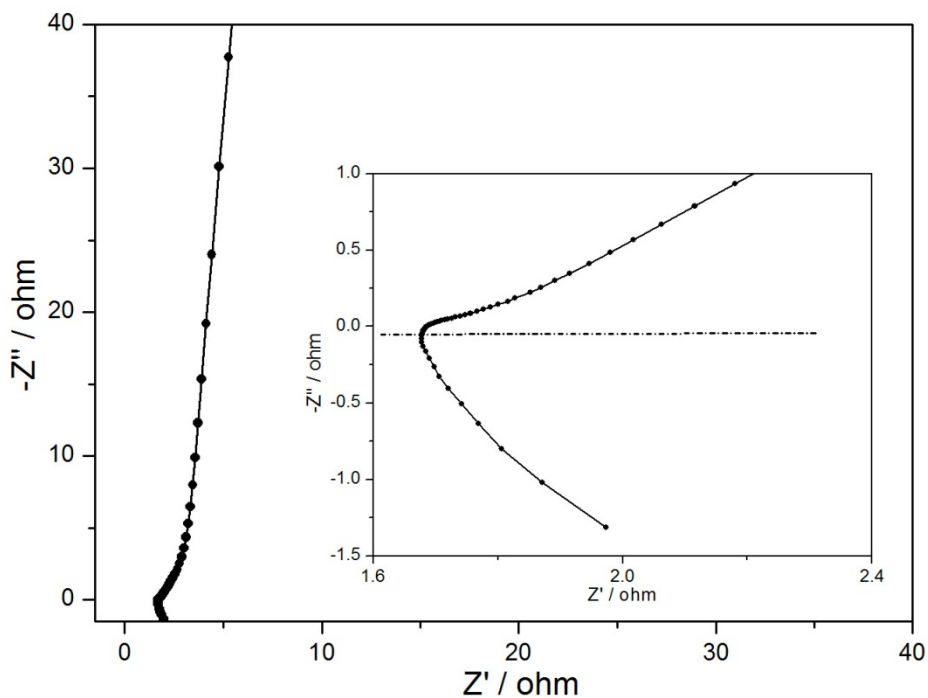


Fig. S6 EIS plot of the Ni foam-supported Zn-Co hydroxide electrode. The inset is an enlarged curve of the high frequency region.

The EIS data shows a solution resistance R_s (the resistance of the KOH aqueous solution, the intrinsic resistance of the electroactive materials, the contact resistance of material with substrate) and a charge-transfer resistance R_{ct} . A vertical line leaning to imaginary axis represents the value of R_s . As can be seen from the inset, R_s can be found to be only 1.68 Ω , indicating that a tightly-coupled interfacial contact exists between the Zn-Co hydroxide nanoflakes and the nickel foam current collector. In the low frequency region, the slope of the impedance plot almost tends to a vertical asymptote, suggesting an ideal capacitor. At high frequency region, it displays a negligible semicircle, revealing the low charge transfer resistance (R_{ct}). The R_{ct} value is merely 0.03 Ω according to the semicircular arc diameter. This result reveals that Zn-Co hydroxide network structure can provide ideal pathway for ion and electron transport.

Table. S2 Specific capacitances and capacitance retention of layered zinc-cobalt hydroxide nanoflakes/Ni foam in this study, compared with some other hydroxides electrodes reported in previous literature.

Electrode structure	Specific capacitance ($F \cdot g^{-1}$)	Capacitance retention
Layered zinc-cobalt hydroxide nanoflakes/Ni foam (this study)	901 $F \cdot g^{-1}$ at 5 $A \cdot g^{-1}$	74.5% from 5 to 30 $A \cdot g^{-1}$
Zinc-cobalt hydroxide film (ref. 5)	160~170 $F \cdot g^{-1}$ at ~0.6 $A \cdot g^{-1}$	———
α -Co(OH) ₂ long nanowire arrays/graphite (ref. 6)	642.5 $F \cdot g^{-1}$ at 1 $A \cdot g^{-1}$	51.5% from 1 to 20 $A \cdot g^{-1}$
CoAl layered double hydroxides nanosheet arrays/Ni foam (ref. 7)	780 $F \cdot g^{-1}$ at 50 $mA \cdot cm^{-2}$ (~5 $A \cdot g^{-1}$)	72.4% from 5 to 50 $mA \cdot cm^{-2}$
NiAl layered double hydroxide/Ni foam (ref. 8)	701 $F \cdot g^{-1}$ at 0.5 $A \cdot g^{-1}$	23.4% from 0.5 to 5 $A \cdot g^{-1}$
CoAl layered double hydroxide nanosheet arrays/platinum films/Ni foam (ref. 9)	734.4 $F \cdot g^{-1}$ at 3 $A \cdot g^{-1}$	60.6% from 3 to 25 $A \cdot g^{-1}$
Petal-like NiAl layered double hydroxide/Ni foam (ref. 10)	795 $F \cdot g^{-1}$ at 0.5 $A \cdot g^{-1}$	27.7% from 0.5 to 10 $A \cdot g^{-1}$
CoAl layered double hydroxide /poly(3,4-ethylenedioxythiophene) nanoplate array/Ni foam (ref. 11)	672 $F \cdot g^{-1}$ at 1 $A \cdot g^{-1}$	67% from 1 to 40 $A \cdot g^{-1}$

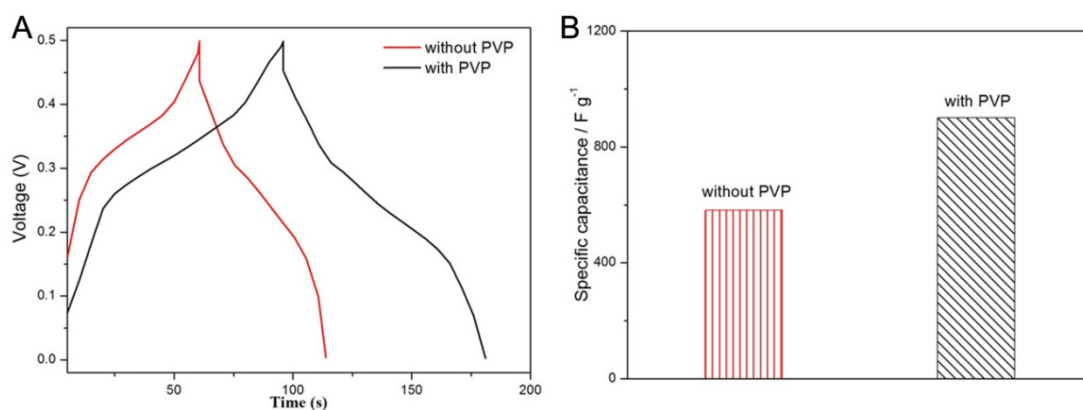


Fig. S7 (A) Charge-discharge curves at $5 \text{ A}\cdot\text{g}^{-1}$ and (B) specific capacitance for the products obtained with and without PVP.

The electrochemical performances of impure Zn-Co hydroxide nanoflakes were investigated. Fig. S7 shows the charge-discharge performance of the product prepared with and without PVP, which were carried out at a galvanostatic current density of $5 \text{ A}\cdot\text{g}^{-1}$ in the potential range of 0-0.5V. Fig. S7A illustrates the charge-discharge curves of the products. In the whole potential region, the charge curves exhibited symmetry to corresponding discharge counter parts, reflecting their supercapacitive behaviors. Fig. S7B shows the specific capacitances of Zn-Co hydroxide at $5 \text{ A}\cdot\text{g}^{-1}$, which were measured from charge-discharge curves from Fig. S7A. The specific capacitances were approximate 582 and $901 \text{ F}\cdot\text{g}^{-1}$, respectively. The product obtained without PVP displayed the relatively low specific capacitance probably was mainly ascribed to the impurity, which decreased the conductivity and hindered electron transmissions.

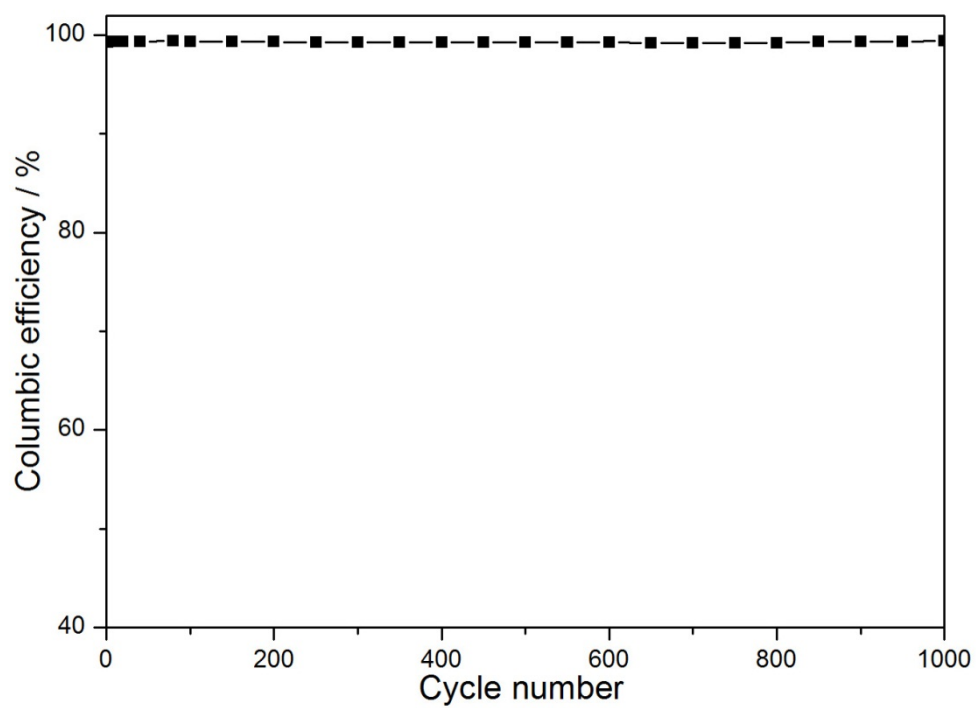


Fig. S8 Columbic efficiency during the cycling test.

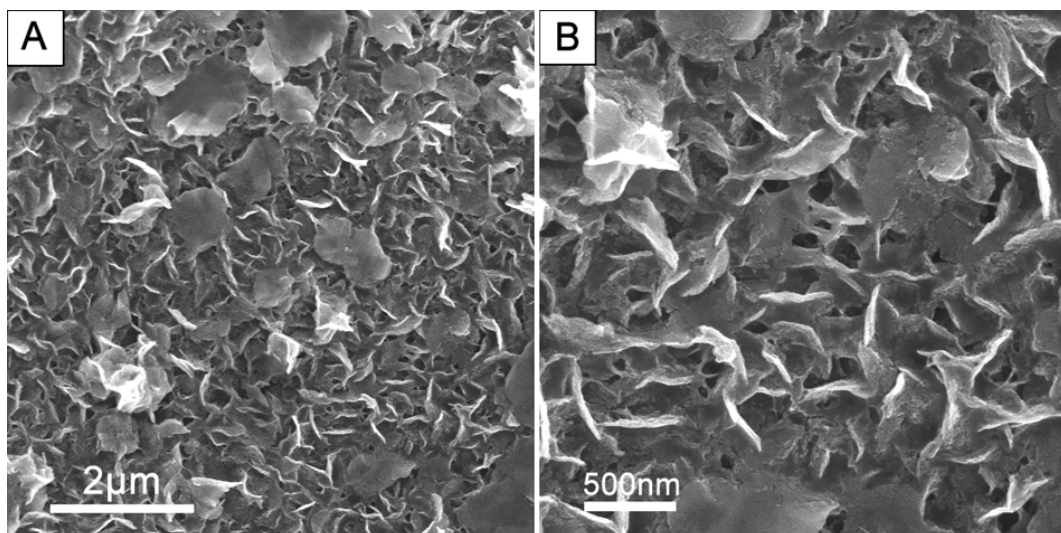


Fig. S9 (A-B) SEM images of the Zn-Co hydroxide nanoflakes on Ni foam after cycling for 1000 cycles with a current density of $5 \text{ A}\cdot\text{g}^{-1}$.

References

- 1 M. Shao, M. Wei, D. G. Evans and X. Duan, *Chem. Commun.*, 2011, **47**, 3171.
- 2 J. Liu, X. Wang, X. Yao, J. Wang and Z. Liu, *Particuology*, 2012, **10**, 24.
- 3 X. Zou, A. Goswami and T. Asefa, *J. Am. Chem. Soc.*, 2013, **135**, 17242.
- 4 L. Cao, F. Xu, Y. Y. Liang and H. L. Li, *Adv. Mater.*, 2004, **16**, 1853.
- 5 M. A. Woo, M.S. Song, T. W. Kim, I. Y. Kim, J.Y. Ju, Y. S. Lee, S. J. Kim, J.H. Choy and S.J. Hwang, *J. Mater. Chem.*, 2011, **21**, 4286.
- 6 J. Jiang, J. Liu, R. Ding, J. Zhu, Y. Li, A. Hu, X. Li and X. Huang, *ACS Appl. Mater. Interfaces*, 2011, **3**, 99.
- 7 Z. Lu, W. Zhu, X. Lei, G. R. Williams, D. O'Hare, Z. Chang, X. Sun and X. Duan, *Nanoscale*, 2012, **4**, 3640.
- 8 J. Wang, Y. Song, Z. Li, Q. Liu, J. Zhou, X. Jing, M. Zhang and Z. Jiang, *Energ. Fuel*, 2010, **24**, 6463.
- 9 J. P. Cheng, J. H. Fang, M. Li, W. F. Zhang, F. Liu and X. B. Zhang, *Electrochim. Acta*, 2013, **114**, 68.
- 10 B. Wang, Q. Liu, Z. Qian, X. Zhang, J. Wang, Z. Li, H. Yan, Z. Gao, F. Zhao and L. Liu, *J. Power Sources*, 2014, **246**, 747.
- 11 J. Han, Y. Dou, J. Zhao, M. Wei, D. G. Evans and X. Duan, *Small*, 2013, **9**, 98.